

# Mid infrared emission of nearby Herbig Ae/Be stars<sup>\*</sup>

R. Siebenmorgen<sup>1</sup>, T. Prusti<sup>2</sup>, A. Natta<sup>3</sup>, T.G. Müller<sup>2</sup>

<sup>2</sup> European Southern Observatory, Karl-Schwarzschildstr. 2, D-85748 Garching b. München, Germany

<sup>2</sup> ISO Data Centre, Astrophysics Division, ESA, Villafranca del Castillo, P.O. Box 50727, E-28080 Madrid, Spain

<sup>3</sup> Osservatorio Astrofisico di Arcetri, Largo E. Fermi 5, I-50125 Firenze, Italy

Received 8 May 2000; accepted 21 June 2000

**Abstract.** We present mid IR spectro-photometric imaging of a sample of eight nearby ( $D \leq 240$  pc) Herbig Ae/Be stars. The spectra are dominated by photospheric emission (HR6000), featureless infrared excess emission (T Cha), broad silicate emission feature (HR5999) and the infrared emission bands (HD 97048, HD 97300, TY CrA, HD 176386). The spectrum of HD179218 shows both silicate emission and infrared emission bands (IEB). All stars of our sample where the spectrum is entirely dominated by IEB have an extended emission on scales of a few thousand AU ( $\sim 10''$ ). We verify the derived source extension found with ISOCAM by multi-aperture photometry with ISOPHT and compare our ISOCAM spectral photometry with ISOSWS spectra.

**Key words:** circumstellar matter – star: pre-main sequence – ISM: lines and bands

## 1. Introduction

The mid-infrared spectrum of Herbig Ae/Be stars is rich in information that can be used to improve our understanding of the circumstellar environment. The wavelength interval between 6 and 13  $\mu\text{m}$  contains most of the infrared emission bands (IEB), as well as the broad silicate feature centered at about 9.7  $\mu\text{m}$ .

From ground-based and KAO spectroscopy (Roche et al. 1991, Schutte et al. 1990) it is known that IEB exist in the spectra of some Herbig Ae/Be stars. A large number of Herbig Ae/Be stars have been measured with the Infrared Space Observatory (ISO). The ISO sample will allow us to determine the properties and nature of the IEB carriers with unprecedented accuracy (Waelkens et al. 1996). These data will be crucial in solving the puzzle of the mid-infrared energetics of Herbig Ae/Be stars, by determining to what extent IEB emission contributes to

the observed mid-infrared luminosity, and how much IR emission comes from a circumstellar disk in Herbig stars of different spectral type and age (Kenyon & Hartmann 1991, Hillenbrand et al. 1992, Natta et al. 1993).

A very important contribution to our understanding of the IEB and of their role in Herbig Ae/Be stars is provided by spatial information on the extension and distribution of the emission at various wavelengths. For example, Prusti et al. (1994) were able to infer the presence of infrared emission bands (IEB) and to determine some of the properties of the distribution of the carriers around Herbig Ae/Be stars from multi-aperture photometry in the three narrow-band filters N1, N2 and N3. Natta & Krügel (1995), using the radiation transfer code developed by Siebenmorgen et al. (1992), computed the expected intensity profile in the IEB and in the adjacent continuum as a function of the spectral type of the exciting star and of the surrounding shell parameters. However, until recently the scarcity of observed intensity profiles has greatly limited the usefulness of these calculations.

Spectro-photometric imaging observations using the circular variable filters (CVF) of ISOCAM (Cesarsky et al. 1996) are capable of producing the spatial information we want. In addition to the determination of the source size at the various wavelengths, they can also reveal additional emission structures and deviations from spherical symmetry. We present in this paper the results of ISOCAM spectro-photometric, ISOPHT (Lemke et al. 1996) multi-aperture and ISOSWS (de Graauw et al. 1996) grating scan observations of a small sample of Herbig Ae/Be stars that we consider particularly suited to this purpose.

Our sample includes 5 stars of spectral type B9/A0 (HD 179218, HD 176386, TY CrA, HD 97048 and HD 97300). They cover a small age interval, from 1 Myr to  $> 3$  Myr (Table 1). Some of these stars (i.e., TY CrA and HD 97048) are known to have strong IEB features (Roche et al. 1991, Deutsch et al. 1995). In addition, Prusti et al. (1994) could infer from multi-aperture study the presence of IEB for HD176393, HD97048 and HD 97300.

In addition to these 5 stars, we have included in our sample two stars of later spectral type, namely HR 5999 (spectral type A5/7) and T Cha (spectral type G8). The

Send offprint requests to: rsiebenm@eso.org

<sup>\*</sup> Based on observations with ISO, an ESA project with instruments funded by ESA Member States (especially the PI countries: France, Germany, the Netherlands and the United Kingdom) with the participation of ISAS and NASA.

aim was to check the dependence of IEB band shapes and intensity profiles on the spectral type of the exciting star. Ground-based observations in the  $10\ \mu\text{m}$  region (Wooden 1994) seem to indicate that, as expected, IEB are weak or absent in Herbig Ae/Be stars of later spectral type (see also the  $3.3\ \mu\text{m}$  survey of Brooke et al. 1993). Much more surprisingly, it was also found that the silicate feature appears in emission only in stars of later spectral types. There is no obvious reason why silicate emission should disappear in hotter stars. Its absence is probably due to the geometrical distribution of the dust around the star. If we believe that the silicate emission is linked to the existence of a circumstellar disk (Chiang & Goldreich 1997), it is possible that early-type stars do not show the silicate feature because they do not have disks. This would confirm the results obtained with millimeter interferometry, namely that Herbig stars of spectral type A show evidence of disks while very few Herbig B stars do (Di Francesco et al. 1994). It is possible that silicate emission disappears in B stars as they age, dissipating their disks and pushing farther away the residual envelopes. The discovery of "transitional" objects, showing both IEB and silicate emission would be very interesting in this context.

A convincing answer to these questions requires a statistical (i.e. large) sample of spectra and intensity maps for Herbig Ae/Be stars of different spectral type and age. However, we feel that our results can provide interesting clues to a possible answer.

This paper contains in Sect. 2 a description of the observations and data reduction techniques. The results for the individual stars are presented and discussed in Sect. 3. A summary is given in Sect. 4.

## 2. Observations

Spectro-photometric images have been obtained with ISOCAM for the stars in our sample in a number of CVF wavelength intervals, selected to probe the emission in IEB at  $6.2$ , " $7.7$ ",  $8.6$  and  $11.3\ \mu\text{m}$ . Additionally, one interval was chosen around the peak of the silicate feature at  $9.7\ \mu\text{m}$ . Typically, we have taken 25 exposures of  $2.1\ \text{s}$  at each CVF wavelength. We used a gain of 2 and the lens providing  $3''$  pixel field of view. The basic data reduction steps are described in Siebenmorgen et al. (1999). After dark current subtraction, glitch removal and flux transient correction, the exposures are coadded in each CVF step. Photometry is obtained applying the spectral response function. After background subtraction we simulate multi-aperture photometry on the images.

In order to understand the photometric uncertainty of this procedure we analyzed data of the calibration star  $\delta$  Draconis and compared it with the Kurucz model. The largest uncertainty was found in the overlap region of CVF1 and CVF2 and is typically of the order of  $\leq 5\%$ . The aperture sequence allows us to determine the full width at half maximum flux (FWHM). For a point source ( $\delta$  Dra-

conis, as shown in Fig. 1), we derive in the wavelength range considered, typical sizes of  $3$ – $4''$  (FWHM) with an uncertainty of about half a pixel size ( $\sim 1.5''$ ).

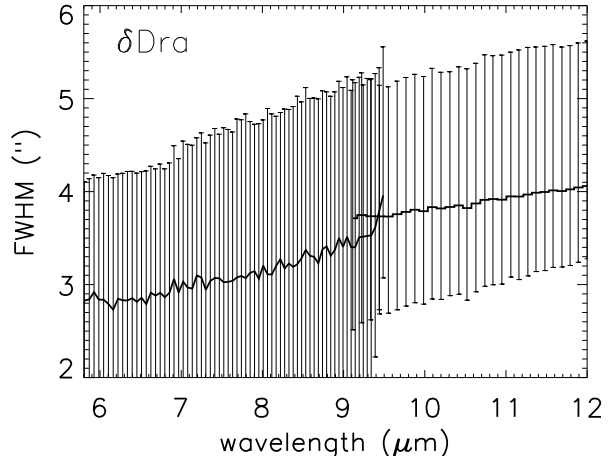


**Fig. 1.** The size (FWHM) of the comparison star  $\delta$  Dra as derived from multi-aperture photometry on the CVF images.

We searched in the ISO archive and whenever possible we compared our ISOCAM spectral photometry with ISOSWS data. The ISOSWS spectra are from the off-line processing version 8.6 (Leech et al. 2000).

The CVF images are contaminated by ghosts and stray light. In order to independently check the FWHM as derived by ISOCAM we compare them to results obtained by ISOPHT. We selected multi-aperture photometry (PHT04, Laureijs et al. 2000) in 11 apertures ranging from  $5''$  up to  $180''$  at an integration time of 32s per filter. The dark subtracted, deglitched and linearised signals of our target stars are compared to an identical PHT04 sequence measured on a point source (HR7127). Such a direct comparison is necessary because the point sources do not exactly follow the theoretical PSF behaviour (Müller 2000). However, adequate point source sequences exist only in a limited number of filters, in practice we can present our PHT04 measurements only at  $7.3\ \mu\text{m}$ .

## 3. Results for Individual Stars

The stars in our sample are listed in Table 1. Column 1 gives the name of the star, Column 2 the spectral type, Column 3 the distance, Column 4 the star effective temperature, Column 5 the luminosity, Column 6 the age and in Column 7 we note the molecular cloud to which the star belongs. Distances, effective temperatures, luminosities and ages are taken from van den Ancker et al. (1996). For TY CrA, for which no Hipparcos distance is available, we have taken the same distance as of HD 176386

**Table 1.** *Our ISO sample of Herbig Ae/Be stars*

Name	ST	Distance (pc)	T (K)	L ( $L_{\odot}$ )	Age (Myr)	Cloud
(1)	(2)	(3)	(4)	(5)	(6)	(7)
HD 97048	A0	$180^{+30}_{-20}$	10000	41	>2	Chamaeleon I
HD 97300	B9	$188^{+43}_{-30}$	10715	37	>3	Chamaeleon I
HD 179218	B9	$244^{+70}_{-44}$	10715	316	0.1	no apparent cloud
HD 176386	B9IV	$140^{+30}_{-20}$	10715	49	2	Corona Australis
TY CrA	B9	$140^{+30}_{-20}$	10715	98	1	Corona Australis
HR 5999	A5-7III/IV	$210^{+50}_{-30}$	7943	85	0.5	Lupus 3
HR 6000	B6 V	$241^{+60}_{-41}$	12882	263	>0.5	Lupus 3
T Cha	G8	$66^{+19}_{-12}$	5888	1.3	>13	Chamaeleon I/II

and computed the luminosity from the observed V, (B-V) (Shevchenko et al. 1993), corrected for extinction with the assumption that the ratio of selective-to-total extinction is  $R=5.1$  (Bibo et al. 1992). The age of the star is then derived by comparing its location on the HR diagram to the evolutionary tracks of Palla & Stahler (1993). The same procedure has been used to estimate the luminosity and age of HR 6000. This procedure is similar to that used by van den Ancker et al. (1996).

### 3.1. HD 97048 and HD 97300

These two stars are located in the Chamaeleon I cloud, and have very similar properties. Their spectral type is A0 (HD 97048) and B9 (HD 97300); they have luminosities of 40 and 37  $L_{\odot}$ , respectively and lie very close to the ZAMS. Both stars have been detected by IRAS. HD 97048 has a near-infrared excess, while HD 97300 has not.

The mid-infrared spectrum of HD 97048 is known to be rich in IEB from ground-based and KAO observations (Roche et al. 1991, Schutte et al. 1990; Brooke et al. 1993). Prusti et al. (1994) found that the emission was extended in both sources (by comparing aperture photometry between 5'' to 16''), but more so in HD 97300 than in HD 97048. Our ISOCAM and a ISOSWS spectrum of HD 97048 is shown in Fig. 2. It is indeed dominated by IEB emission centered at 6.2, "7.7", 8.6 and 11.3  $\mu\text{m}$ . HD 97048 is extended on scales of a few arcseconds (5–10''). Consequently the ISOSWS spectrum (Van Kerckhoven et al. 1999), which is flux calibrated assuming a point source, underestimates the total emission; its high spectral resolution shows that the "7.7"  $\mu\text{m}$  band is due to two separate components, which are unresolved by ISOCAM.

A deeper full CVF scan combined with photometric mid IR images of HD97300 has been presented by us in a separate paper (Siebenmorgen et al. 1998). It was found that the complete mid IR spectrum of the source is dominated by a huge ring structure of about 7500 AU in size.

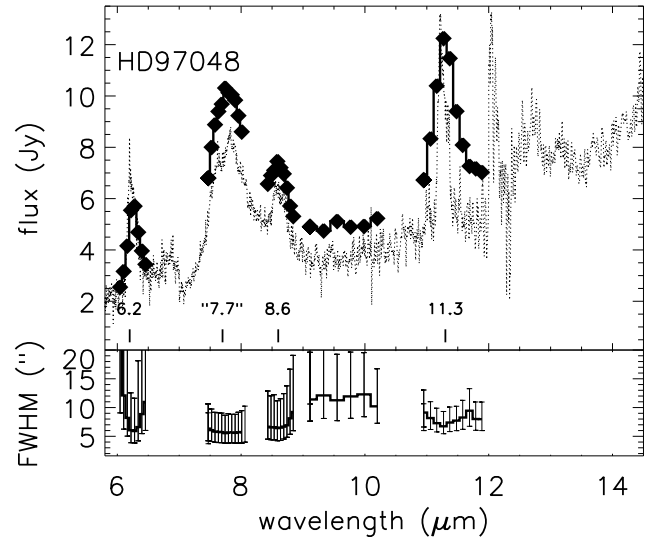


**Fig. 2.** Top: Mid infrared spectrum of HD97048. The ISO-CAM CVF spectrum is indicated by  $\diamond$  and connected by the solid line. The ISOSWS spectrum is shown by the dotted line. Bottom: The FWHM as derived from multi-aperture photometry on the CVF images.

It was proven, by means of a dust model including transiently heated particles, that all the ring emission is due to the IEB carriers. The amount of circumstellar matter was found to be rather small ( $\sim 0.03 M_{\odot}$ ). In Fig. 3 we compare the full CVF wavelength spectrum with the observing strategy of sparse CVF scans, presented in this paper. One notices that the absolute photometry of both observations are identical down to a few %. Good agreement is also found for the derived FWHM of both CVF scans. We derive a FWHM of 13–19'', which gives a clear sign of a huge extended nebulae as was independently verified by stray light free, narrow band ISOCAM images.

The FWHM of  $14 \pm 3''$  as derived from our ISOPHT multi-aperture sequence at 7.3  $\mu\text{m}$ , presented in Fig. 4, is consistent with the CVF results.

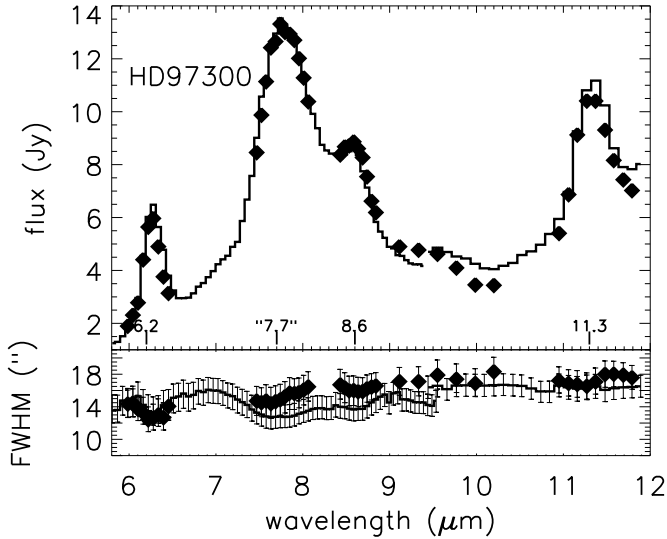


**Fig. 3.** Top: Mid infrared spectrum of HD97300. The CVF full scan by Siebenmorgen et al. (1998) is shown as solid line and the CVF sparse scan of this paper by ( $\diamond$ ). Bottom: The FWHM as derived from multi-aperture photometry on the CVF full scan (line) and sparse scan ( $\diamond$ ).

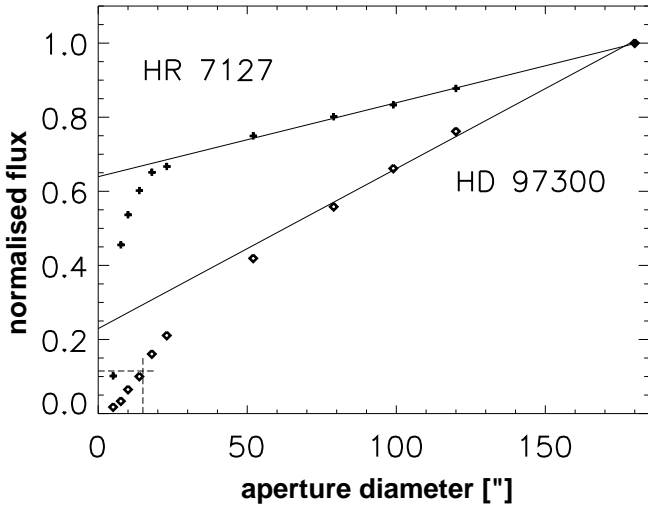


**Fig. 4.** ISOPHT multi-aperture sequence on a point source (HR 7127) and the extended source HD 97300 at  $7.3 \mu\text{m}$ . The line indicate the background estimate and the intersection at  $0''$  gives the source flux. The dashed line shows for HD 97300 the distance at half the source flux (FWHM). The FWHM of HD 97300 as determined from this figure is  $14 \pm 3''$ .

### 3.2. TY CrA and HD 176386

The triple system TY CrA (spectral type B9 of the primary) and the binary HD 176386 (spectral type B9 of the primary) are located in the Corona Australis molecular cloud. The stars are separated from each other by about

$55''$ . Both stars are located very close to the ZAMS. Both have been detected by IRAS, but show no near-infrared excess, if anomalous extinction is taken into account (Bibo et al. 1992). TY CrA has been detected at 1.3 mm, but the amount of circumstellar matter associated to it is quite small (Hillenbrand et al. 1992; Natta et al. 1997). The mid-infrared spectrum of TY CrA was measured in a small aperture ( $4''$ ) by Roche et al. (1991), who found strong IEB. Multi-aperture photometry of HD 176386 by Prusti et al. (1994) indicate extended emission.

In Fig. 5 we show the morphology at  $11.28 \mu\text{m}$ . At about  $8''$  SE from the peak we see a bar like structure (TY CrA bar). The bar is not caused by stray-light or ghost components, which can be predicted with the optical model of ISOCAM. The spectrum of the spherical component of TY CrA is shown in Fig. 6. Photometry was done in half circle apertures centered on the star at the opposite side of the bar. This flux was multiplied by two to get an estimate of the total flux without the bar component. This procedure gives an estimate of the flux in the spherically symmetric envelope around the star. The spectrum is rich in IEB and has a very pronounced  $8.6 \mu\text{m}$  band. The  $11.05 \mu\text{m}$  feature detected by Roche et al. (1991) is not resolved by ISOCAM but clearly present in both ISOSWS spectra (Corporon et al. 1999). The source is very extended ( $\sim 2000 \text{ AU}$ ) in both the IEB and the continuum. Consequently the absolute flux in both ISOSWS spectra is underestimated by  $\sim 40\%$ .

In order to deduce the spectrum of the bar like component we have mirrored the pixels in the half circle used for  $41''$  aperture photometry and subtracted these images from the original background cleaned maps. The spectrum of the TY CrA bar is shown in Fig. 7. It shows again strong IEB but weaker  $7.7''$  and  $8.6 \mu\text{m}$  bands as compared to the spherical component of TY CrA.

As in TY CrA, we see two peaks of emission also in HD 176386. The maximum brightness is at the stellar position. Photometry of the spherical component was done with half circles in a similar manner as for TY CrA. The spectrum is rich in IEB. The band ratios are quite similar to the bar component of TY CrA (Fig. 8). The FWHM as derived from the ISOCAM images are indicative of a large extended halo. They are confirmed by the ISOPHOT multi-aperture measurements at  $7.3 \mu\text{m}$ . In Fig. 10 we show the ISOPHT measurements of HD 176386. For apertures above  $80''$  the signals are strongly contaminated by the adjacent source TY CrA. We derive a source size of  $9 \pm 3''$  (FWHM) for HD 176386 and  $13 \pm 3''$  (FWHM) for TY CrA (Fig. 11). Both size estimates are consistent with the CVF results.

In order to derive photometry of the second component of HD 176386, we mirrored the pixels of the half circle  $41''$  aperture and subtracted the result maps from the original background cleaned images. The spectrum of the second peak, "HD 176386 bar", is computed in a  $14''$  aperture. The source is clearly detected at all wavelengths (Fig. 9). Its spectral shape, in particular of the  $6.2''/7.7''$  band ra-

tios, are quite different from the HD176386 main component (Fig. 8) but similar to TY CrA main component and HD97048 (Fig. 2).

### 3.3. HD 179218

HD 179218 (also called MWC 614) is a young star of spectral type B9. It is listed as a Herbig Ae/Be star by Thé et al. (1994). It has no companion down to a distance of  $0.4''$  (Pirzkal et al. 1997). To the best of our knowledge, it has not been observed in the near-infrared, but has IRAS fluxes in the four bands and shows a  $10\ \mu\text{m}$  emission feature in the low-resolution IRAS spectra.

The multi-aperture CVF spectrum is shown in Fig. 12. There are pronounced IEB visible at  $6.2$ ,  $7.7$  and  $8.6\ \mu\text{m}$  on top of a strong silicate emission feature. As discussed by Waelkens et al. (1999) the silicate band of HD179218 is dominated by substructures due to crystallinity. Those are absent in spectra of the interstellar medium or in the disks of the youngest stellar objects. We do not find any clear sign of an extended structure in the ISOCAM or in the ISOPHT observations. As expected for a point-like sources, the ISOSWS photometry is in line with our ISOCAM spectrum.

### 3.4. HR 6000 and HR 5999

HR 6000 and HR 5999 form the proper motion binary system Dunlop 199. They are located in the Lupus 3 star forming region which is at a distance of  $140 \pm 20\ \text{pc}$  (Hughes et al. 1993). Van den Ancker et al. (1996) classified HR6000 as a young main sequence object with spectral type B6. The strong X-ray emission is accounted for by a T Tauri companion (Zinnecker & Preibisch 1994). We have a detection of HR 6000 above the background level. The star is close to the much brighter target HR 5999 so that only the central five pixels could be used to deduce the spectrum shown in Fig. 13. By comparing the spectrum with a black body of  $13000\ \text{K}$ , we notice that it is featureless.

The pre-main sequence star HR 5999 (also called V856 Sco) has spectral type A7 III (Thé et al. 1994) and has Rossiter 3930 as companion (Stecklum et al. 1995), which probably accounts for the strong X-ray emission. HR 5999 has a strong near-IR excess (Hillenbrand et al. 1992), and has been detected by IRAS at  $12$ ,  $25$  and  $60\ \mu\text{m}$ , as well as at millimeter wavelengths (Henning et al. 1994). The amount of circumstellar matter associated to the star is of the order of  $0.006\ M_{\odot}$ . Our mid-infrared spectrum of HR 5999 (Fig. 14) shows clearly a broad silicate emission feature. In the CVF spectrum this feature peaks at considerably shorter wavelengths ( $\approx 9.6\ \mu\text{m}$ ) than observed for HD179218 or Elias 1 (Hanner et al. 1994). Its intensity is small in comparison to the underlying continuum, with a ratio of the peak – to – continuum flux of about 1.4. The FWHM as derived by the ISOCAM

CVF images or the ISOPHT multi-aperture sequence of HR6000 and HR5999 is typical for point sources.

### 3.5. T Cha

T Chamaeleonis is a T Tauri star of spectral type G8 (Alcalá et al. 1993) and the coolest star in our sample. It is superposed on a dark cloud DC 300.2–16.8 between the star forming Chamaeleon I and II clouds. Although a priori the later spectral type suggests that it is physically more difficult to excite transiently heated particles, we considered this star suitable for our sample as its presumed parent cloud DC 300.2–16.8 shows an unusually high amount of excess radiation in the mid-infrared (Lau-reijs et al. 1989).

The Hipparcos distance to T Cha is  $66_{-12}^{+19}\ \text{pc}$ . This is considerably closer than the estimated distances to the Chamaeleon I ( $160 \pm 15$ ) and II ( $178 \pm 18$ ) pc clouds (Whit-tet et al. 1997). On the other hand, Terranegra et al. (1999) associate T Cha to a moving group of pre-main sequence stars which have the same radial velocity as the CO gas in DC 300.2–16.8. They note, however, that despite sharing a common proper motion with the group, T Cha has a deviating radial velocity measured by Covino et al. (1997). Therefore, unfortunately, it is not possible to make any firm statements of the possible physical connection between T Cha and DC 300.2–16.8.

The spectrum of T Cha is featureless, with no indication of IEB or silicate emission (Fig. 15). The continuum we measure is about a factor 4–5 larger than the expected photospheric flux (about  $0.2\ \text{Jy}$  at  $6\ \mu\text{m}$ ), possibly due to a circumstellar disk (Alcala et al. 1993). Given the lack of dust features it is not a surprising result that there is no extended mid-infrared emission around T Cha. Also the ISOPHT multi-aperture sequence is for apertures below  $23''$  consistent with the point source HR7127. It is possible that a G8 star cannot excite extended mid-infrared emission. However, given the fact that the connection to DC300.2-16.8 is uncertain, we cannot exclude that the lack of extended IEB emission is simply due to the absence of low-density circumstellar matter associated with the star.

## 4. Conclusions

We find that the mid infrared spectrum of the Herbig Ae/Be stars: HD 97048, HD 97300, TY CrA and HD 176386, is dominated by IEB and show no signature of silicate emission. All those stars have an extended halo on scales of up to a few thousand AU. Two of the stars (TY CrA and HD 176386) have a secondary peak of emission at distances of about  $1000\ \text{AU}$  from the main component. A secondary peak is found also in HD97300 and in addition, there is emission in an elliptical ring structure at a much larger scale ( $\sim 7500\ \text{AU}$  from the star).

The IEB ratios in the secondary peaks show differences when compared to those of the central regions. This can be

explained as being due to differences of the excitation of transiently heated particles and variations of the column density (Siebenmorgen et al. 1998).

The other targets of our sample are at distances similar to the IEB dominated objects. They remain point like at the spatial resolution of ISO ( $\sim 5''$  at  $6\mu\text{m}$ ). Two of those stars (HR6000 and T Cha) show featureless mid IR spectra while the other objects (HR5999 and HD 179218) have a pronounced silicate emission bump. Because silicate grains are much larger particles than the IEB carriers (Siebenmorgen et al. 1992), they are not transiently heated and therefore must be located close to the star, most likely in a disk component. This interpretation is in agreement with the compact emission detected. The mid IR spectrum of HD 179218 shows both silicate emission and IEB; nevertheless it is not extended. Consequently the detection of IEB alone is not a clear indicator to assume an associated extended emission structure of more than a few hundred AU.

Although the ISOCAM CVF has a known stray-light component we could confirm the deduced sizes (FWHM) by ISOPHT multi-aperture photometry. We find that the total flux is in the ISOSWS spectra of the extended sources systematically underestimated. This is expected because the ISOSWS flux calibration assumes a point source. For point like sources we derive for both ISO instruments a set of consistent photometric flux density values.

*Acknowledgements.* PIA is a joint development by the ESA Astrophysics Division and the ISOPHOT consortium. The ISOCAM data presented in this paper was analysed using "CIA", a joint development by the ESA Astrophysics Division and the ISOCAM Consortium. The ISOCAM Consortium is led by the ISOCAM PI, C. Cesarsky.

## References

- Alcalá J.M., Covino E., Franchini M., et al., 1993, A&A 272, 225
- Bibo E.A., Thé P.S., Dawanas D.N., 1992, A&A 260, 293
- Brooke T.Y., Tokunaga A.T., Strom S.E., 1993, ApJ 106, 656
- Cesarsky C., Abergel A., Agnès P. et al., 1996, A&A 315, L32
- Chiang E.I., Goldreich P., 1997, ApJ 480, 368
- Corporon P., Ceccarelli C., Lagrange A.-M., 1999, "The Universe as seen by ISO", P.Cox & M.F. Kessler (eds.), ESA SP-427, p. 297
- Covino E., Alcalá J.M., Allain S., et al., 1997, A&A 328, 187
- de Graauw Th., Haser L.N., Beintema D.A., et al., 1996, A&A 315, L49
- Deutsch L.K., Hora J.L., Butner H.M., Hoffman W.F., Fazio G.G., 1995, ApSS 224, 361
- Di Francesco J., Evans N.J.II, Harvey P.M., Mundy L.G. Butner H.M., 1994, ApJ 432, 710
- Hanner M.S., Brooke T.Y., Tokunaga A.T., 1994, ApJ 433, L97
- Henning Th., Launhardt R., Steinacker J., Thamm E., 1994, A&A 291, 546
- Hillenbrand L.A., Strom S.E., Vrba F.J., Keene J., 1992 ApJ 397, 613
- Hughes J., Hartigan P., Clampitt L., 1993, AJ 105, 571
- Kenyon S.J., Hartmann L.W., 1991, ApJ 383, 664
- Laureijs R.J., Chlewicki G., Clark F.O., Wesselius P.R., 1989, A&A 220, 226
- Laureijs R.J., Klass U., Richards P.J., et al., 2000, "ISO Handbook Volume V (PHT)", SAI-99-069/Dc, <http://www.iso.vilspa.esa.es/>
- Leech K., De Graauw T., van den Ancker M., et al., 2000, "ISO Handbook Volume VI (SWS)", SAI-2000-008/Dc, <http://www.iso.vilspa.esa.es/>
- Lemke D., Klaas U., Abolins J., et al., 1996, A&A 315, L64
- Müller T.G., "ISOPHOT Aperture Sequences on Point- and Extended Sources", ISO beyond point sources: studies of extended infrared emission, Proceedings, ESA Publication SP-455, Laureijs, Leech, & Kessler (eds.), 2000
- Natta A., Krügel E., 1995, A&A 302, 849
- Natta A., Prusti T., Krügel E., 1993, A&A 275, 527
- Natta A., Grinin V.P., Mannings V., Ungerechts H., 1997, ApJ 491, 885
- Palla F., Stahler S.W., 1993, ApJ 418, 414
- Pirzkal N., Spillar E.J., Dyck H.M., 1997, ApJ 481, 392
- Prusti T., Natta A., Palla F., 1994, A&A 292, 593
- Roche P.F., Aitken D.K., Smith C.H., 1991, MNRAS 252, 282
- Schutte W.A., Tielens A.G.G.M., Allamandola L.J., Cohen M., Wooden D.H., 1990, ApJ 360, 577
- Shevchenko V.S., Grankin K.N., Ibragimov M.A., et al., 1993 ApSS 202, 121
- Siebenmorgen R., Krügel E., Mathis J.S., 1992, A&A 266, 501
- Siebenmorgen R., Natta A., Krügel E., Prusti T., 1998, A&A 339, 134
- Siebenmorgen R., Blommaert J., Sauvage M., Starck J.-L., 1999, "ISO Handbook Volume III (CAM)", SAI-99-057/Dc, <http://www.iso.vilspa.esa.es/>
- Stecklum, B., Eckart A., Henning Th., Löwe M., 1995, A&A 296, 463
- Terranegra L., Morale F., Spagna A., Massone G., Lattanzi M.G., 1999, A&A 341, L79
- Thé P.S., de Winter D., Perez M.R., 1994, A&AS 104, 315
- Van Kerckhoven, Tielens A.G.G.M., Waelkens C., 1999, "The Universe as seen by ISO", P.Cox & M.F. Kessler (eds.), ESA SP-427, p. 421
- van den Ancker M.E., de Winter D., Thé P.S., 1996, A&A 313, 517
- Waelkens C., Waters L. B. F. M., De Graauw M. S., et al., 1996, A&A 315, 245.
- Waelkens C., Malfait K., Waters L. B. F. M., De Graauw M. S., et al., 1999, "The Universe as seen by ISO", P.Cox & M.F. Kessler (eds.), ESA SP-427, p. 607
- Wooden D.H., 1994, Astronomical Society of the Pacific Conference Series, Vol. 62, P. S. Thé, M. R. Perez, and E. P. J. Van den Heuvel (eds.), p.138
- Whittet D.C.B., Prusti T., Franco G.A.P., et al., 1997, A&A 327, 1194
- Zinnecker H., Preibisch T., 1994, A&A 292, 152

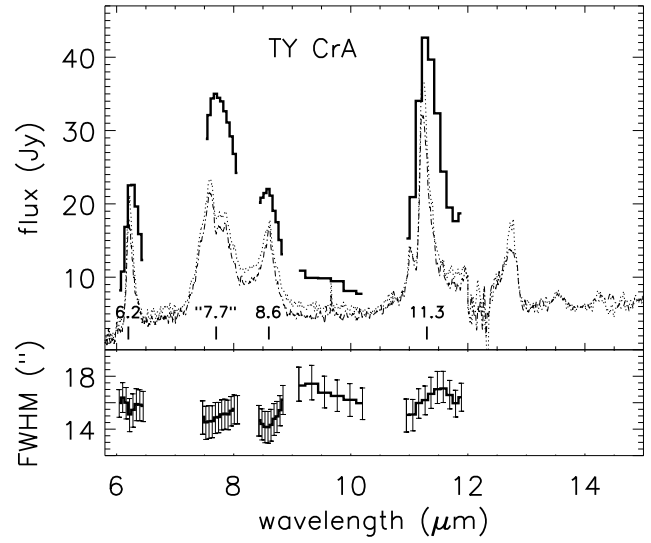


**Fig. 6.** Top: Mid infrared spectrum of the spherical component around TY CrA. The CVF scan is shown as solid line and the ISOSWS spectra of two different epochs are indicated by the dotted and dashed lines. Bottom: The FWHM as derived from multi-aperture photometry on the CVF images.

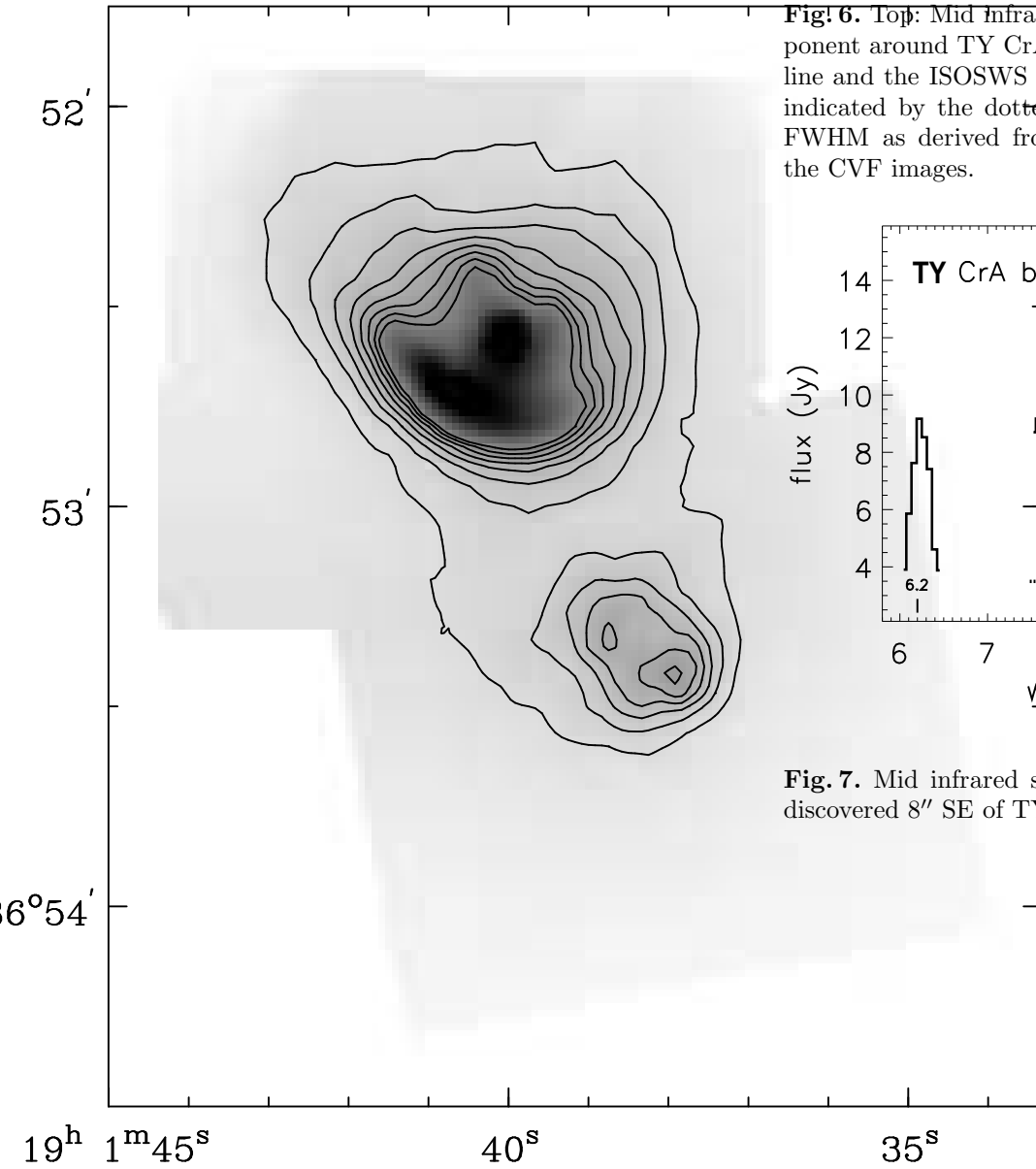


**Fig. 7.** Mid infrared spectrum of the bar like structure discovered 8'' SE of TY CrA.

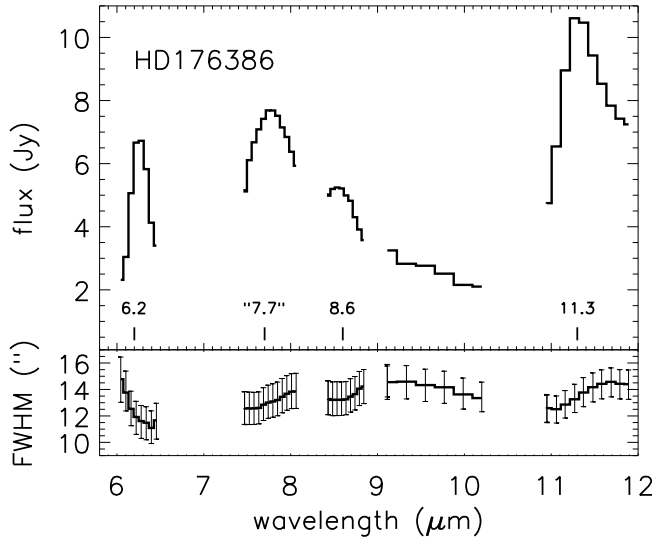


**Fig. 8.** Top: Mid infrared spectrum of HD 176386 main component. Bottom: The FWHM as derived from multi-aperture photometry on the CVF images.

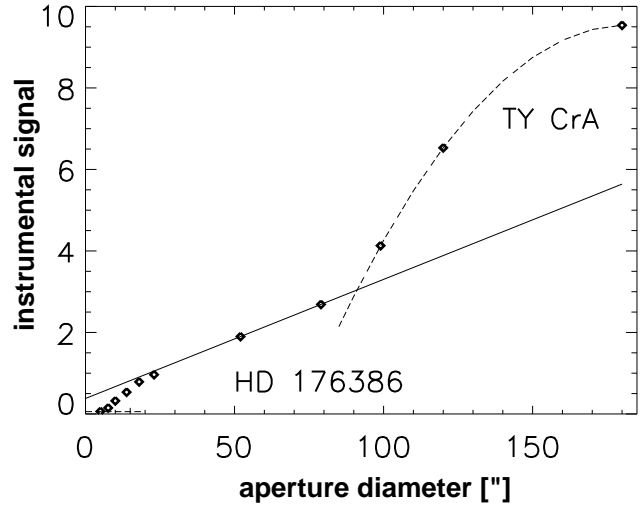


**Fig. 10.** ISOPHT multi-aperture sequence at  $7.3 \mu\text{m}$  on HD 176386. For apertures larger than  $80''$  the adjacent source TY CrA dominates the measured signals (Fig. 5).

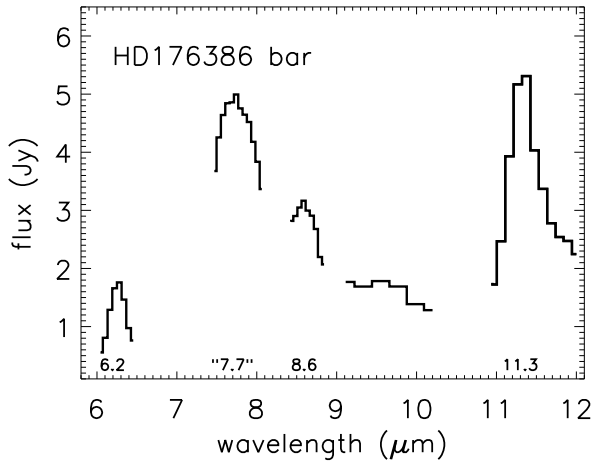


**Fig. 9.** Mid infrared spectrum of the second component of HD 176386.

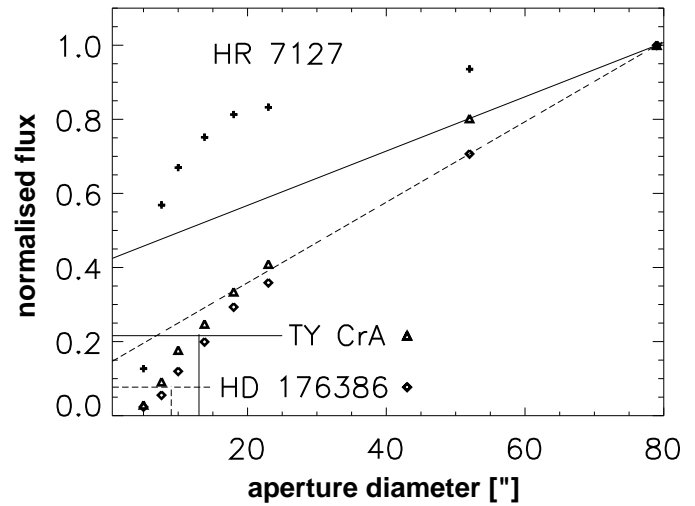


**Fig. 11.** ISOPHT multi-aperture sequence, normalised flux at  $7.3 \mu\text{m}$  on a point source (HR 7127) and on the extended adjacent sources TY CrA and HD 176386. The full and dashed line are for TY CrA and HD 176386, respectively. The FWHM is deduced as in Fig. 4 and determined to  $13 \pm 3''$  (TY CrA) and  $9 \pm 3''$  (HD 176386).

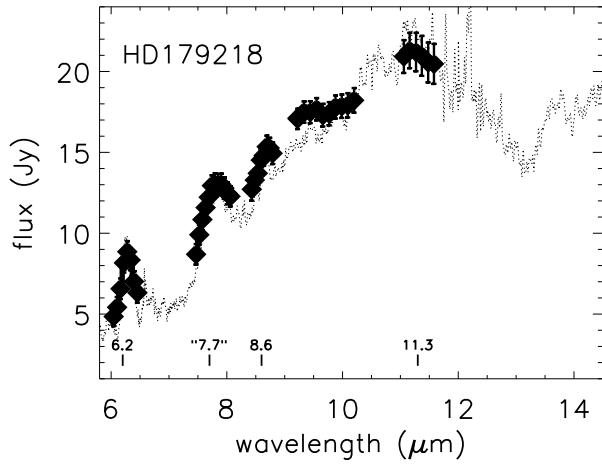


**Fig. 12.** Mid infrared spectrum of HD179218. The CVF scan is shown as solid line and the ISOSWS spectra by the dotted line.

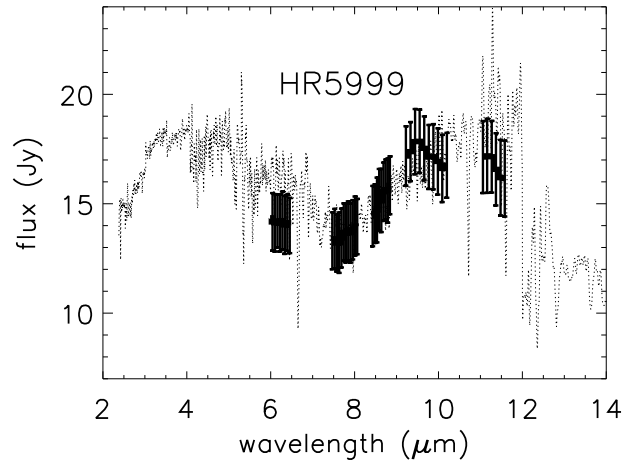


**Fig. 14.** As Fig. 12 for HR 5999.

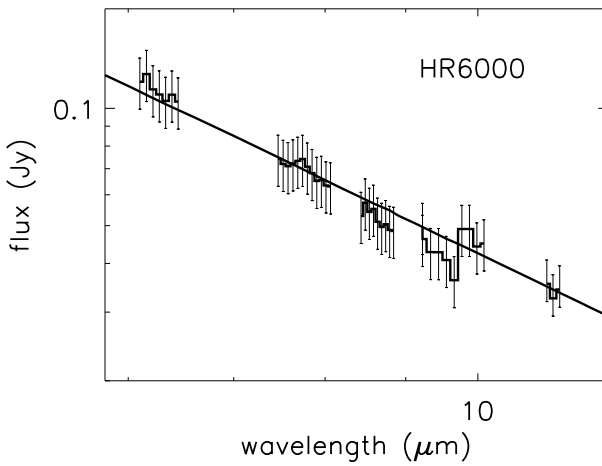


**Fig. 13.** Mid infrared spectrum of HR 6000 together with a black-body spectrum of 13000 K (solid line).

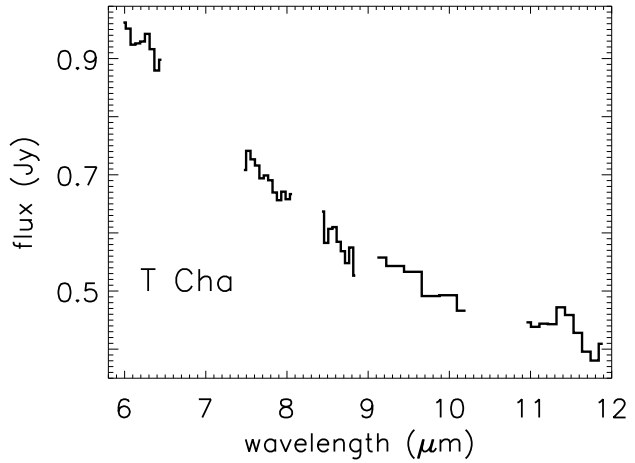


**Fig. 15.** Mid infrared spectrum of T Cha.